Food and Chemical Toxicology 67 (2014) 26–34

Contents lists available at ScienceDirect

Food and Chemical Toxicology

journal homepage: www.elsevier.com/locate/foodchemtox

Multiple pathways are involved in palmitic acid-induced toxicity

Eun-Jung Park [a], Ah Young Lee [b], Sungjin Park [b], Jae-Ho Kim [a], Myung-Haing Cho [b,c,d,e,*]

[a] Department of Molecular Science and Technology, Ajou University, Suwon 443-749, Republic of Korea
[b] Laboratory of Toxicology, College of Veterinary Medicine, Seoul National University, Seoul 151-742, Republic of Korea
[c] Graduate School of Convergence Science and Technology, Seoul National University, Suwon 443-270, Republic of Korea
[d] Graduate Group of Tumor Biology, Seoul National University, Seoul 110-799, Republic of Korea
[e] Advanced Institute of Convergence Technology, Seoul National University, Suwon 443-270, Republic of Korea

ARTICLE INFO

Article history:
Received 16 November 2013
Accepted 14 January 2014
Available online 28 January 2014

Keywords:
Palmitic acid
Toxicity
Apoptosis
Autophagy
ER stress
Mitochondria

ABSTRACT

In this study, we identified the toxic mechanism following the accumulation of palmitic acid (PA), a saturated fatty acid, in human Chang liver cells. After PA exposure for 24 h, the mitochondria and the endoplasmic reticulum (ER) became dilated, and lipid droplets and organelles were observed within autophagosomes. Cell viability decreased with an ATP reduction and the G2/M phase arrest. The expression of SOD-2, but not of SOD-1, markedly increased after PA exposure, which also elevated the number of cells generating ROS. PA enhanced the levels of proteins related to apoptosis, necroptosis, autophagy, and ER stress. Moreover, the inhibition of caspases, p53, necroptosis, or ER stress substantially rescued PA-induced cytotoxicity and, similarly, the inhibition of caspases and ER stress counteracted PA-induced changes in the cell cycle. Conversely, the inhibition of necroptosis and p53 signaling accelerated the changes in the cell cycle triggered by PA exposure. Blocking autophagy exacerbated PA-induced cytotoxicity and alterations in the cell cycle and caused disappearance of cellular components. These results suggest that PA induces apoptosis accompanied by autophagy through mitochondrial dysfunction and ER stress, which are triggered by oxidative stress in Chang liver cells and that blocking autophagy accelerates cell damage following PA exposure.

1. Introduction

Fatty acids can be classified into unsaturated and saturated fatty acids depending on the presence and absence of carbon–carbon double bonds, respectively. Fatty acids serve as key sources of fuel because they produce large quantities of ATP. However, excessive accumulation of fatty acids may induce a cellular toxic response known as "lipotoxicity" through an increase of free fatty acids in the body, and thus cause a variety of diseases such as liver disease, type 2 diabetes, insulin resistance, atherosclerosis, and coronary heart disease (Gaggini et al., 2013; Murea et al., 2010; Leamy et al., 2013; Loria et al., 2013). Saturated and unsaturated fatty acids have been reported to induce distinct cellular responses under the same conditions, however, saturated fatty acids have been found to be more harmful to health than unsaturated fatty acids (Ricchi et al., 2009; Mei et al., 2011; Schönfeld and Wojtczak, 2008).

The liver is a central organ in metabolism that serves multiple functions such as protein synthesis, glycogen storage, hormone production, and detoxification. In these regards, liver cells are rich in organelles that facilitate such functions, including the endoplasmic reticulum (ER), mitochondria, and lysosomes. Furthermore, the coordination and functional crosstalk of these organelles are crucial for maintaining cellular calcium levels and homeostasis, as well as for regulating cell survival and cell death (Chen and Yin, 2011; Kim et al., 2006; Ferri and Kroemer, 2001; Smaili et al., 2013). For example, the ER is involved in protein synthesis, lipid metabolism, carbohydrate metabolism, and detoxification. Proteins that are misfolded or immature are translocated from the ER into lysosomes and digested, and the accumulation of misfolded or immature proteins in the ER lumen or the cytosol can cause apoptotic cell death by mitochondrial dysfunction.

Palmitic acid (PA) is the most common saturated fatty acid found in animals, plants, and microorganisms, and PA overloading is known to induce apoptotic cell death by triggering ER stress (Gu et al., 2010; Zhang et al., 2012; Cao et al., 2012). However, the mechanism underlying PA toxicity remains incompletely understood. In this study, we investigated the mechanism by which accumulated PA produces toxicity in the human Chang liver cell line (Chang cells).

* Corresponding author at: Laboratory of Toxicology, College of Veterinary Medicine, Seoul National University, Seoul 151-742, Republic of Korea. Tel.: +82 2 880 1276; fax: +82 2 873 1268.
E-mail address: mchotox@snu.ac.kr (M.-H. Cho).

http://dx.doi.org/10.1016/j.fct.2014.01.027
0278-6915/

2. Materials and methods

2.1. Cell culture

Chang cells, which were established using HeLa cells, were kindly provided by Dr. SJ Kim (CHA University, Seoul, Korea). The cells were maintained in Dulbecco's modified Eagle's medium (DMEM) containing 10% heat-inactivated fetal bovine serum (FBS), penicillin (100 IU/mL), and streptomycin (10 μg/mL). Cells were grown and maintained in 10 cm^2 cell culture plate at 37 °C in a humidified incubator with 5% CO_2.

2.2. PA preparation

PA was conjugated to bovine serum albumin (BSA) as described previously (Choi et al., 2009). Briefly, PA (Sigma–Aldrich, St. Louis, MO, USA) was conjugated to 5% BSA at a 3:1 M ratio by adding a 20 mM solution of PA in phosphate-buffered saline (PBS) and incubating at 70 °C until solubilization, which was facilitated by the drop-wise addition of 1 N NaOH. The fatty acid soap was conjugated with fatty acid-free BSA in PBS to achieve the appropriate 3:1 (albumin-to-PA) molar ratio, and the final concentration was set at 5 mM.

2.3. Cell viability and cell cycle analysis

Cell viability was measured using the 3-(4-5-dimethylthiazol-2-yl)-2,5-diphenyltetrazolium bromide (MTT, Sigma–Aldrich) assay. Cells were seeded in 96-well tissue culture plates at a density of 5×10^3 cells/well. After stabilization overnight, the cells were treated with 31.25, 62.5, 125, and 250 μM of PA for 24 h. MTT solution (2 mg/mL) was added and the cells were incubated for 3 h more at 37 °C. The cells were then solubilized, and the absorbance was measured at 540 nm by a microplate spectrophotometer (VersaMax, Molecular Devices, Sunnyvale, CA, USA). The viability of the treatment group was expressed as a percentage of the control group, which was considered as 100%. To examine the cell cycle, cells were fixed using 70% ethanol after 24-h exposure to PA and then stained with propidium iodide and RNase (Sigma–Aldrich). The cell cycle was analyzed by measuring the DNA content in cells using the FACSCalibur system and CellQuest software (BD Biosciences, Franklin Lakes, NJ, USA) (Park et al., 2010, 2008).

2.4. Lipid droplet assay

The lipid droplets in cells were measured using a commercial kit according to the manufacturer's protocols (Cayman Chemical Co., Ann Arbor, MI, USA). Briefly, cells were harvested after exposure for 24 h with designated concentrations. After centrifuging at 800×*g* for 5 min, cells were resuspended in fixative solution at room temperature (RT) for 10 min. After washing, the cell pellet was resuspended in Nile red staining solution at RT for 15 min, and the cells were then analyzed at an excitation wavelength of 488 nm by using the FACSCalibur system and CellQuest software (BD Biosciences).

2.5. Reactive oxygen species (ROS) measurement

Cells were treated with various concentrations of PA for 24 h, washed with PBS, and then incubated for 30 min with 5 μM of carboxy-2′7′-dichlorodihydrofluorescein diacetate (Invitrogen, Carlsbad, CA, USA). After washing, the cells were resuspended in FBS-free DMEM, and the cells generating ROS were counted using the FACSCalibur system and the results were analyzed using CellQuest software (BD Biosciences).

2.6. ATP measurement

ATP production was measured using a commercial kit (Promega, Fitchburg, WI, USA) according to the manufacturer's protocols. Briefly, cells were seeded at a density of 5×10^3 cells/well in 96-well plates and incubated with various concentrations of PA for 24 h. At the end of the incubation, a volume of CellTiter-Glo® Reagent equal to the volume of the culture medium present in each well was added and the contents were mixed for 2 min on an orbital shaker, and then the mixtures were incubated at RT for 10 min. The luminescence of the solutions was measured using a microplate luminometer (Berthold Technologies, Bad Wildbad, Germany).

2.7. Immunohistochemistry and observation

Cells (3×10^3/well) were seeded in 2-well chamber slides and stabilized for 24 h. After exposure to PA, the cells were fixed in 4% paraformaldehyde (PFA) for 15 min at RT. After washing, the cells were fixed again with ice-cold methanol at −20 °C and then blocked for 1 h using 3% BSA in Tris-buffered saline (10 mM Tris, pH 8.0, and 150 mM NaCl) containing 0.05% Tween-20 (TBST). The cells were next incubated overnight at 4 °C with primary antibodies (1:100 dilution) against p62, NRF-2, superoxide dismutase (SOD)-1, and SOD-2 (Santa Cruz Biotechnology Inc., Santa Cruz, CA, USA), CHOP and calnexin (Cell Signaling Technology, Danvers, MA, USA), and lysosome-associated membrane protein (LAMP)-2 (Abcam, Cambridge, MA, USA), and then incubated with Alexa Fluor 555-conjugated secondary antibodies (1:200 dilution) for 2 h at RT. Mitochondria were labeled with MitoTracker® Deep Red FM (Invitrogen) for 30 min, and the cells were then fixed in 4% PFA for 15 min at 37 °C. After washing, coverslips were mounted using Fluoroshield™ mounting medium with DAPI (ImmunoBioScience, Mukilteo, WA, USA). Cells were visualized using a fluorescence confocal laser scanning microscope (LSM710, Carl Zeiss).

2.8. Protein expression analysis

Cells were homogenized in a protein extraction solution (iNtRON Biotech, Kyunggi-do, Korea) and then lysates were collected by centrifugation at 13,000 rpm for 10 min. Protein concentration was measured using the bicinchoninic acid method (Sigma–Aldrich), and then equal amounts of protein were separated on polyacrylamide gels and transferred to nitrocellulose membranes (Hybond ECL; Amersham Pharmacia Biotech, Franklin Lakes, NJ, USA). The membranes were blocked for 1 h at RT with 5% (w/v) non-fat dried milk in TBST and then immunoblotted with the following specific primary antibodies (1:1000 dilution): rabbit polyclonal antibodies against Poly(ADP-ribose) polymerase (PARP), cleaved caspase-9, and light chain 3 (LC3; Cell Signaling Technology), beclin 1, p53, and p62 (Santa Cruz Biotechnology), and receptor-interacting protein (RIP) 3, p-IRE 1 alpha, and autophagy protein 5 (ATG5, Abcam); rabbit monoclonal antibodies against Bcl-2-associated X protein (BAX; Millipore, Milford, MA, USA) and caspase-3, phospho-extracellular signal regulated kinase (p-ERK), perilipin, and phospho-c-Jun N-terminal kinase (p-JNK; Cell Signaling Technology), mouse monoclonal antibodies against Bcl-2 and cytochorme c (Santa Cruz Biotechnology) and RIP1 (R & D System, Minneapolis, MN, USA); and goat polyclonal antibody against β-actin (Santa Cruz Biotechnology). The blots were then incubated with corresponding anti-rabbit, anti-goat, or anti-mouse IgGs conjugated with horseradish peroxidase (1:2000; Santa Cruz Biotechnology), and immunoreactive proteins were detected using an ECL reagent.

2.9. Transmission electron microscopy (TEM)

Cells were incubated for 24 h in the absence or the presence of PA (250 μM). After washing with PBS, the cells were immediately fixed in 2% glutaraldehyde in 0.1 M sodium cacodylate buffer (pH 7.2) for 2 h. Following fixation, the cells were stained for 20 min in 0.5% aqueous uranyl acetate, dehydrated using graded ethanol solutions, and then embedded in Spurr's resin. Thin sections were cut using an ultramicrotome (MT-X, RMC, Tucson, AZ, USA) and stained with 2% uranyl acetate and Reynolds's lead citrate, and then the sections were examined using a LIBRA 120 transmission electron microscope (Carl Zeiss) at an accelerating voltage of 80 kV.

2.10. Statistics

The statistical significance of quantitative results was evaluated using ANOVA and *t* tests, and $p < 0.05$ was considered statistically significant.

3. Results

3.1. Increase in lipid droplets and alteration of cellular components after PA exposure

Cells containing lipid droplets increased dose-dependently after PA exposure. When cells were exposed to 31.25, 62.5, 125, and 250 μM of PA for 24 h, the proportion of cells containing lipid droplets were 2.2 ± 0.4%, 2.7 ± 1.6%, 5.0 ± 0.9%, and 13.0 ± 3.8%, respectively, compared with a control level of 0.7 ± 0.1% (Fig. 1). After the same PA treatments, ATP production decreased to 96.6 ± 1.4%, 95.9 ± 1.2%, 94.2 ± 0.5%, and 92.3 ± 3.0% of control, respectively (Fig. 2A). Moreover, PA altered mitochondrial structure (Fig. 2D) and increased the levels of LAMP-2, a lysosomal membrane protein, and calnexin, an ER membrane protein (Fig. 2B, C, and E).

3.2. Changes in cell viability and in the cell cycle following PA treatment

In preliminary experiments, the average viability of cells that were treated with 500 μM of PA for 24 h was measured to be 31.7% of the control level, and the morphology of cells was noted to be severely damaged. Thus, we determined 250 μM as the maximal concentration of PA to be used (data not shown). When cells

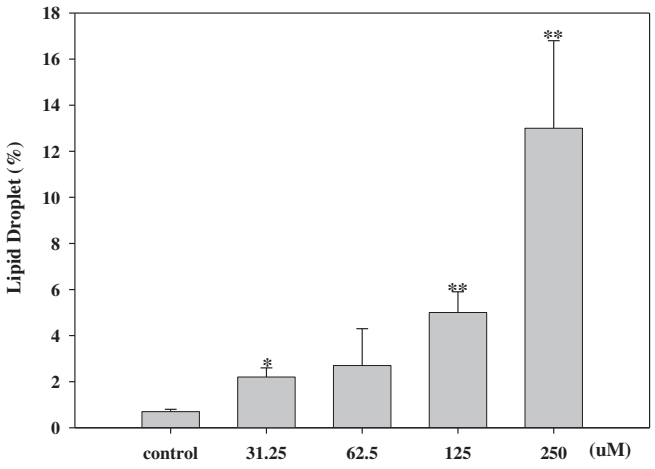

Fig. 1. Increase in lipid droplets following PA exposure. Cells containing lipid droplets were counted using a FACS analysis system. The experiments were performed 3 times, independently, and the results are presented as mean (AV) ± standard deviation (SD); $^{*}p < 0.05$, $^{**}p < 0.01$.

were exposed for 24 h to 31.25, 62.5, 125, and 250 μM of PA, cell viability decreased to 87.4 ± 3.1%, 73.3 ± 6.8%, 66.7 ± 1.5%, and 53.3 ± 1.2% of control, respectively (Fig. 3A). After 24 h exposure, the cell cycle was not affected noticeably by PA up to a concentration of 125 μM, whereas the cell cycle was effectively arrested at the G2/M phase with the addition of 250 μM PA, and this was coupled with an increase in S and subG1 cell fractions (Fig. 3B). Furthermore, the subG1 fraction, which indicates the apoptotic cell population, increased with time (Supple 1).

3.3. Generation of ROS after PA exposure

As shown in Fig. 4A, cells generating ROS increased to 116.2 ± 5.8%, 122.1 ± 1.39%, 135.3 ± 6.5%, and 176.1 ± 1.4% of control when exposed for 24 h to 31.25, 62.5, 125, and 250 μM of PA, respectively. Moreover, the expression of the anti-oxidant protein SOD-2, but not SOD-1, increased considerably in cells exposed to 250 μM PA, as did the expression of NRF-2, a transcription factor that is stimulated in response to oxidative stress (Fig. 4B–D).

3.4. Effect of PA on cell morphology and cellular components

TEM images showed that mitochondria and ER were dilated after PA exposure (Fig. 5, Supple 2) and that lipid droplets and organelles were observed within autophagosomes (Fig. 1B).

3.5. Changes in protein expression after PA exposure

PA treatment increased, in a dose-dependent manner, the levels of caspase-dependent apoptotic cell death-related proteins such as

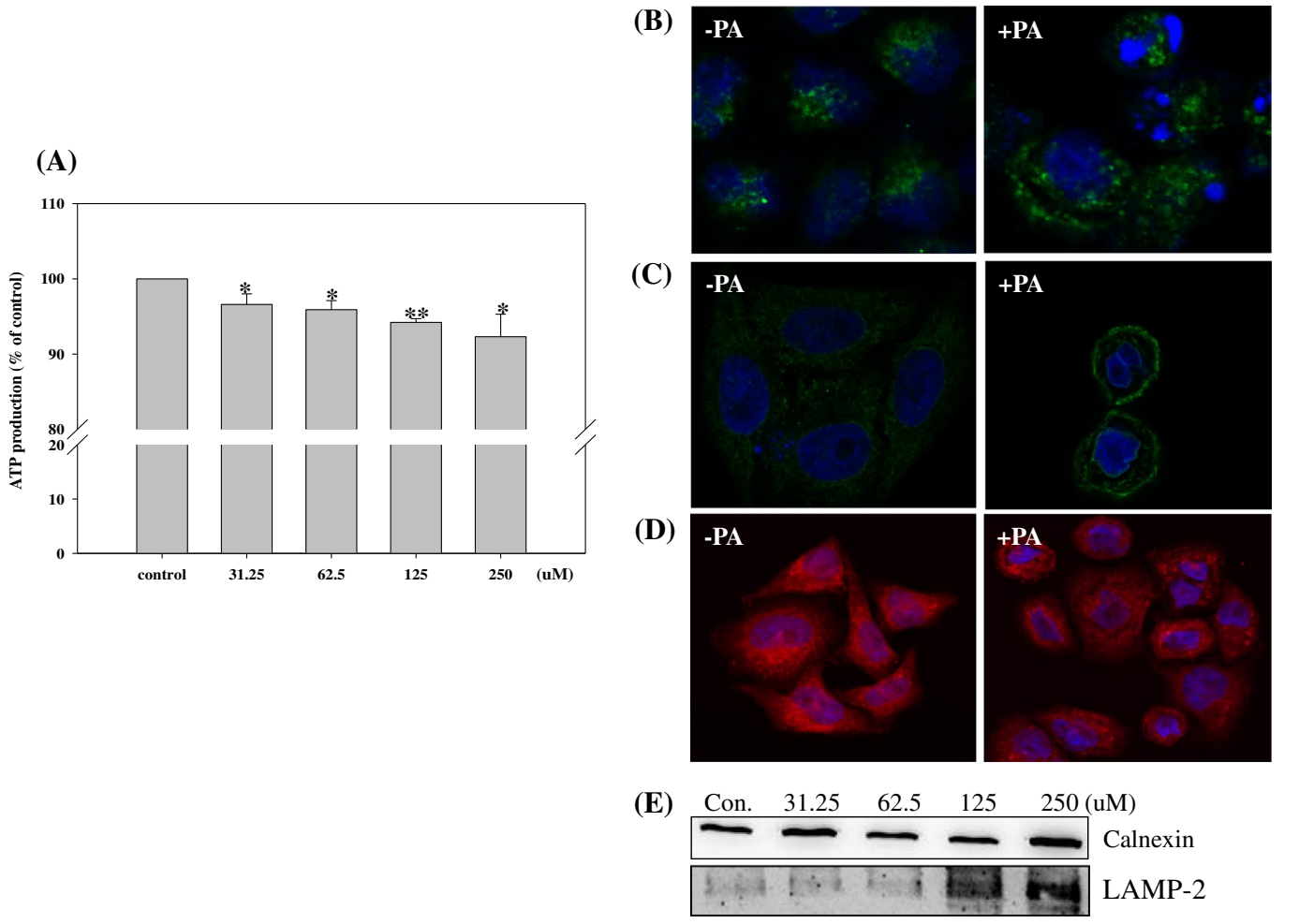

Fig. 2. Changes in cellular components after PA treatment. (A) Decrease in ATP production, $^{*}p < 0.05$. (B–D) Staining of cellular components. Cells were incubated for 24 h with or without 250 μM PA and images were captured at 800× magnification. (B) Lysosome-associated membrane protein (LAMP)-2, (C) calnexin, and (D) mitochondria. (E) Dose-dependent changes in ER and lysosomal membrane proteins.

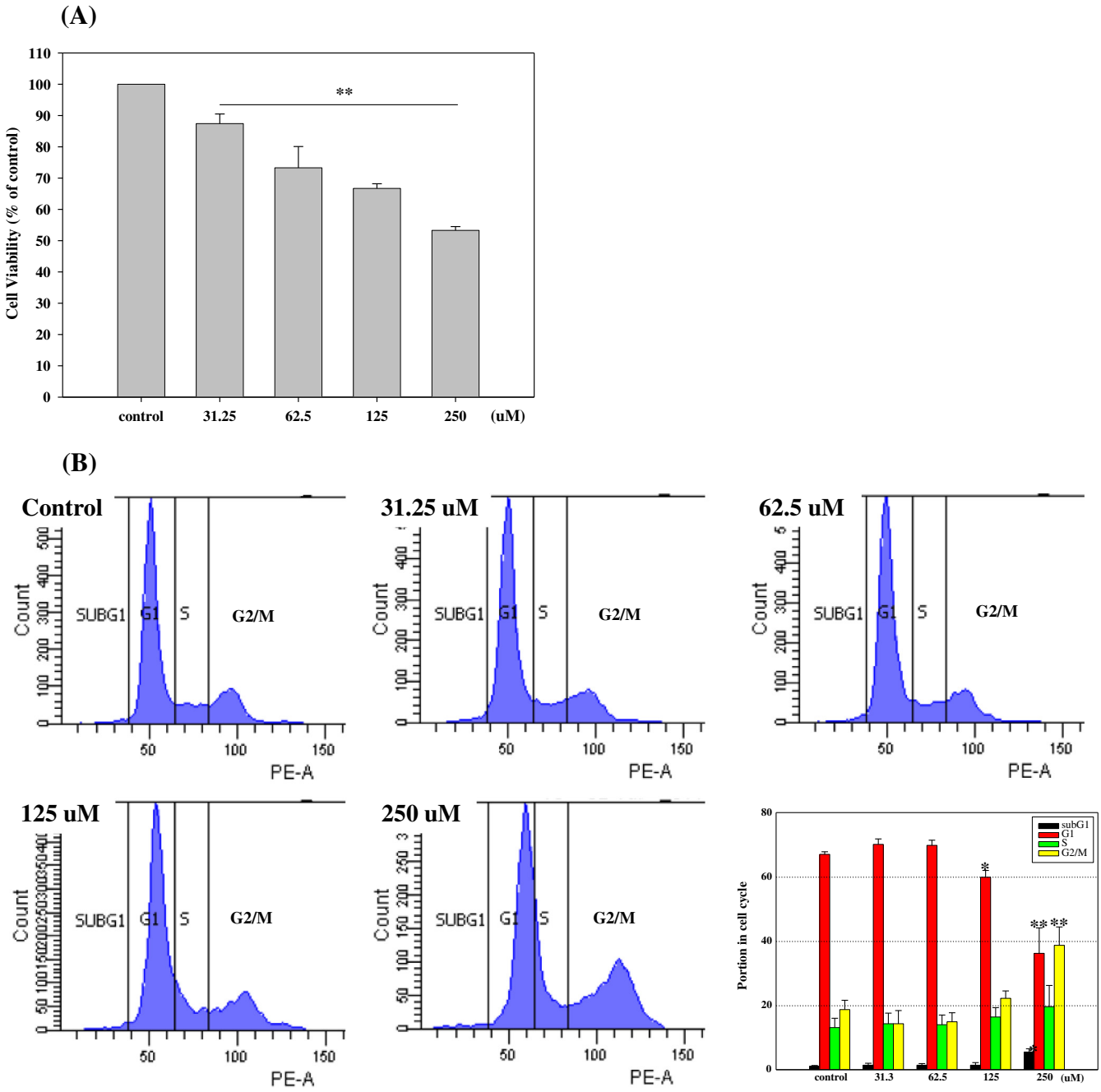

Fig. 3. Alteration in cell viability and in the cell cycle after PA exposure. Cells were treated with the indicated concentrations of PA for 24 h. Results are presented as AV ± SD of 3 independent experiments. $^{*}p < 0.05$, $^{**}p < 0.01$. (A) Cell viability, and (B) cell cycle. The graph shows representative data.

cytochrome *c*, cleaved caspase-9 and caspase-3, and PARP (Fig. 6). Furthermore, after PA exposure, the levels of proteins related to necroptosis (RIP1, RIP3), autophagy (LC3B, p62), and ER stress (CHOP, p-IRE 1 alpha) increased, as did the levels of Bcl-2 and p53. However, the levels of p-ERK (specifically ERK2), p-JNK (specifically JNK1), and beclin1 decreased markedly after treatment with 250 μM PA, and the level of BAX protein did not change substantially (Fig. 6, Supple 3).

3.6. Effect of various inhibitors on cell viability and cell cycle

Multiple pathways were found to be involved in cell death triggered by PA exposure. Thus, we studied further the roles of these pathways by using several inhibitors. PA-induced reduction in cell viability was rescued substantially when cells were pretreated with a caspase inhibitor (Z-VAD-FMK), a p53 inhibitor (pifithrin-alpha), a necroptosis inhibitor (necrostatin-1), or an ER-stress inhibitor (tauroursodeoxycholic acid, TUDCA) (Fig. 7A). The cell cycle changes induced by PA were abolished by pretreatment with the caspase inhibitor and rescued substantially by pretreatment with the ER-stress inhibitor (Fig. 7B), whereas pretreatment with inhibitors of necroptosis and p53 accelerated the PA-induced changes in cell cycle. More importantly, pretreatment with bafilomycin (Baf) A1, an autophagy inhibitor, exacerbated PA-induced cytotoxicity and enhanced PA-induced alterations in the cell cycle. When cells were treated for 1 h with Baf A1 in the absence of PA addition, ER dilatation and autophagosome formation increased markedly (Fig. 8A). Furthermore, when cells were exposed to 250 μM PA

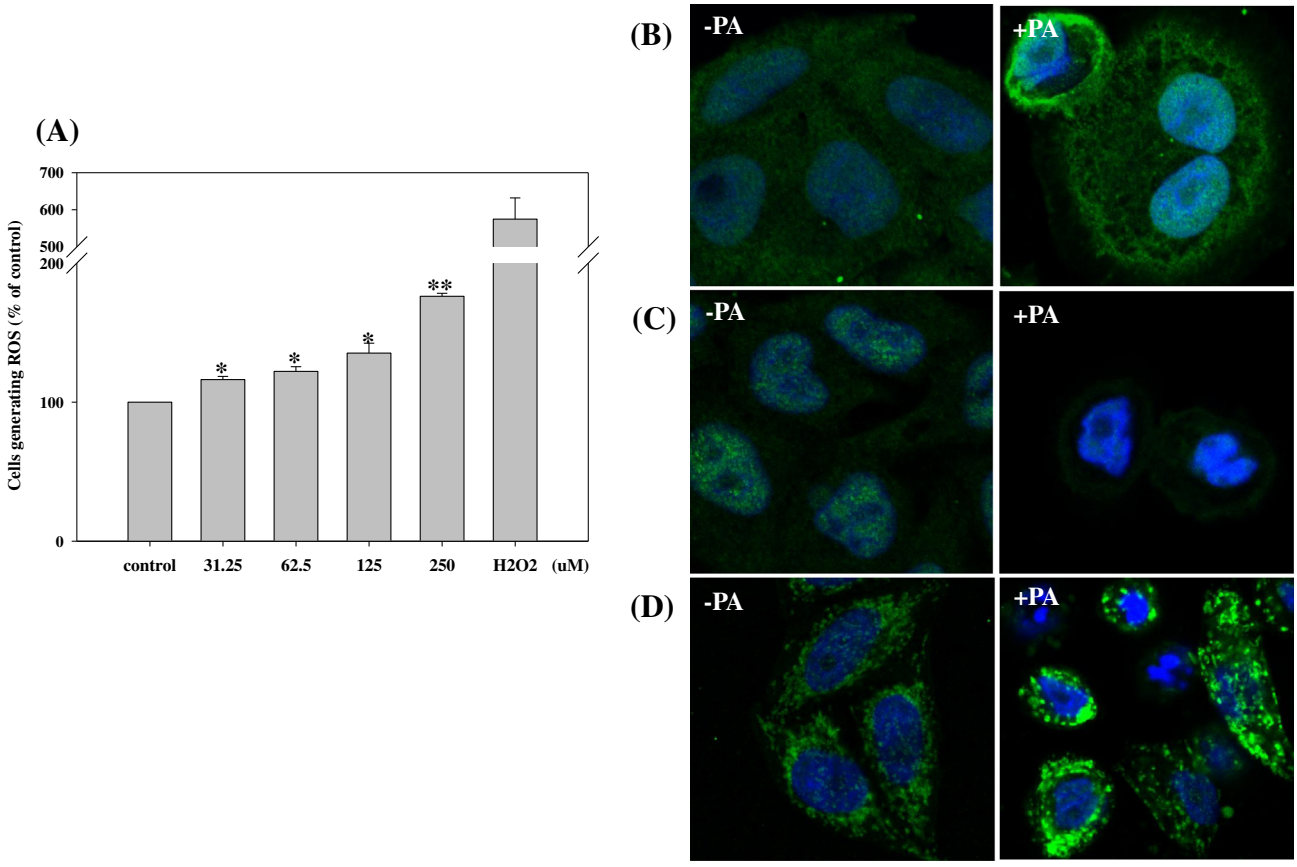

Fig. 4. Increase in ROS following PA exposure. (A) Cells generating ROS were counted using a FACS analysis. The experiments were performed 3 times, independently, and the results of the treatment group were calculated as percentages of the control group (100%). H_2O_2 (1 mM, 30 min) was used as the positive control. $^*p < 0.05$. (B–D) Expression of ROS-related proteins. Cells were incubated for 24 h with or without PA (250 μM) and examined at 800× magnification. (B) NRF-2, (C) SOD-1, and (D) SOD-2.

together with Baf A1 pretreatment, cellular components disappeared or were severely damaged (Fig. 8B), and these changes were coupled with an increase in p62 protein aggregation (Supple 4).

4. Discussion

Intracellular fatty acids are essential components of cells that serve as an energy source, as structural components of membranes, as building blocks for hormone synthesis, and as mediators of cellular signaling. Therefore, maintaining adequate amounts of fatty acids is critical for cellular functions and cell survival (Liu and Czaja, 2013). Cells store fatty acids as lipid droplets, and the anions of fatty acids cannot penetrate the lipid bilayer of mitochondria because of their uncoupling effect (Dedukhova et al., 1991). Thus, cells digest and use lipid droplets through macroautophagy, a type of the lysosomal degradative pathway of lipophagy (Knævelsrud and Simonsen, 2012; Singh and Cuervo, 2012). However, excessive accumulation of fatty acids can cause adverse health effects through a cellular toxic response known as "lipotoxicity." In this study, exposure to PA for 24 h markedly increased lipid droplets in autophagosome-like vacuoles and also elevated the level of the proteins perilipin and LC3B-II (Singh and Cuervo, 2012). However, ATP production did not increase at any of the treatment concentrations even though the cells contained increased levels of lipid droplets.

Functionally, cell death can be induced through programmed and accidental processes, and apoptosis, autophagy, necroptosis, and paraptosis are classified as being part of programmed cell death (Kroemer et al., 2009). These cell death pathways are characterized by unique morphological and biochemical alterations in cells, and analyzing the cell cycle provides a critical clue that helps define the cell death pathway. We found that 24-h exposure to PA up to a concentration of 125 μM did not induce any major changes in the cell cycle, despite reducing cell viability in a dose-dependent manner. However, when cells were exposed to 250 μM PA, the cells detected in the G2/M phase increased, and this was coupled with an elevation in the level of Bcl-2 protein (Basu and Haldar, 1998) and a slight increase in the number of apoptotic cells. Conversely, the levels of p-ERK (in particular ERK2) and p-JNK (in particular JNK1) proteins decreased clearly in cells exposed to 250 μM PA (Liu et al., 2004; Li et al., 2010). PA exposure also induced ER dilatation and an increase of autophagosome-like vacuoles. Cells divide completely into 2 daughter cells during the G2/M phase and the daughter cells share cellular components almost equally, including the nuclear and cytoplasmic materials, organelles, and cell membranes, as well as the DNA in the nucleus (Imoto et al., 2011). Therefore, we hypothesize that the arrest in the G2/M phase following PA exposure is caused by organelle damage and cytosolic vacuolization.

Chang liver cells were established using HeLa cells, which were derived from cervical cancer cells (http://www.atcc.org), and p53, which a tumor suppressor protein, plays a key role in lipid metabolism, cell death pathways, and cell cycle regulation (Lorin et al., 2010; Chaabane et al., 2013; Zhang et al., 2010; Vousden and Ryan, 2009; Moscat and Diaz-Meco, 2009; Jin, 2005). Necroptosis-related proteins such as RIP1 and RIP3 are also activated by death signals from the cell membrane, including TNF alpha and FADD (Wu et al., 2012). In this study, PA exposure increased the levels of p53, RIP1, and RIP3, and pretreating cells with inhibitors of p53 and

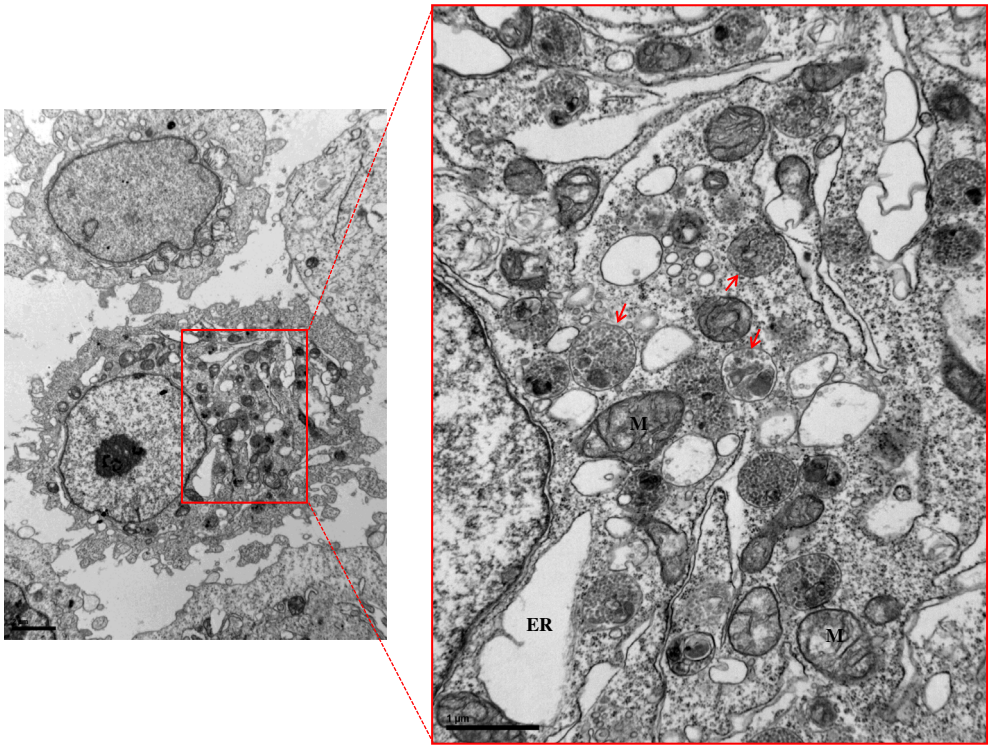

Fig. 5. Morphological changes following PA exposure. TEM images were acquired of cells that had been exposed to 250 μM PA for 24 h. Red arrows indicate phagosomes containing lipid droplets and organelles. ER dilatation and mitochondrial damage triggered by PA treatment can be observed readily. M, mitochondria; ER, endoplasmic reticulum. (For interpretation of the references to color in this figure legend, the reader is referred to the web version of this article.)

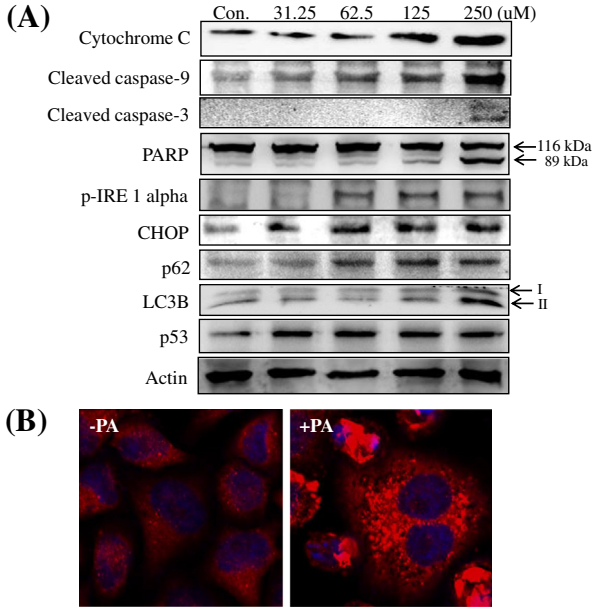

Fig. 6. Changes in protein expression following PA exposure. The experiment was performed 3 times, independently, and all results showed similar trends; representative data are presented. (A) Dose-dependent changes. (B) Increase in the aggregation of p62 protein. Cells were incubated for 24 h without or with PA (250 μM). Magnification 800×.

necroptosis partially rescued the reduction in cell viability induced by PA treatment; however, the addition of these 2 inhibitors accelerated the cell cycle arrest at the G2/M phase.

Apoptosis can be triggered by mitochondrial damage, which is followed by the release of cytochrome *c* and the caspase cascade (Kim et al., 2006). The BAX protein activates mitochondrial release of cytochrome *c* (Renault and Manon, 2011). Apoptosis can be also induced by the dysregulation of cellular homeostasis, and the ER, lysosomes, and the Golgi apparatus are major sites of the cell death signaling triggered by this dysregulation (Ferri and Kroemer, 2001). In this study, PA activated SOD-2, a mitochondrial SOD, but not SOD-1, a cytosolic SOD, and concomitantly increased ROS production, and PA induced apoptosis through the caspase-dependent pathway (Fukai and Ushio-Fukai, 2011). Free fatty acid-induced oxidative stress lowers the rate of mitochondrial β-oxidation, leading to a reduction in cellular ATP content (Liu and Czaja, 2013). Furthermore, PA increased the levels of the ER stress-related proteins such as CHOP and p-IRE 1 alpha and caused ER dilatation. ER stress, which can be triggered by (a) disruptions in redox regulation and calcium regulation, (b) glucose deprivation, and (c) viral infection, leads to the accumulation of unfolded proteins in the ER lumen or the cytosol (Chen and Yin, 2011; Sano and Reed, 2013). TUDCA prevents apoptosis by inhibiting the BAX pathway (Rivard et al., 2007) and ER stress (Lee et al., 2010). Here, the levels of BAX protein did not change markedly in cells exposed to 250 μM PA. Thus, PA-induced cell death, but not the alteration in cell cycle, was rescued completely by TUDCA pretreatment.

Apoptosis and autophagy share multiple regulatory systems and common signaling pathways. Lysosomes contain several catabolic hydrolases that function optimally at an acidic pH and contribute to autophagic cell death, which is induced by signals such as oxidative stress and ER stress (Tanida, 2011). Lysosomes also participate in degrading apoptotic cells present in the heterophagic vacuoles of healthy cells (Ferri and Kroemer, 2001). Defective lysosomal metabolism can cause fatal diseases such as Danon disease, Gaucher's disease types 1 and 3, and Anderson–Fabry disease (Cox and Cachón-González, 2012). In this study, PA exposure increased the aggregation of p62 protein, which is degraded in the lysosome.

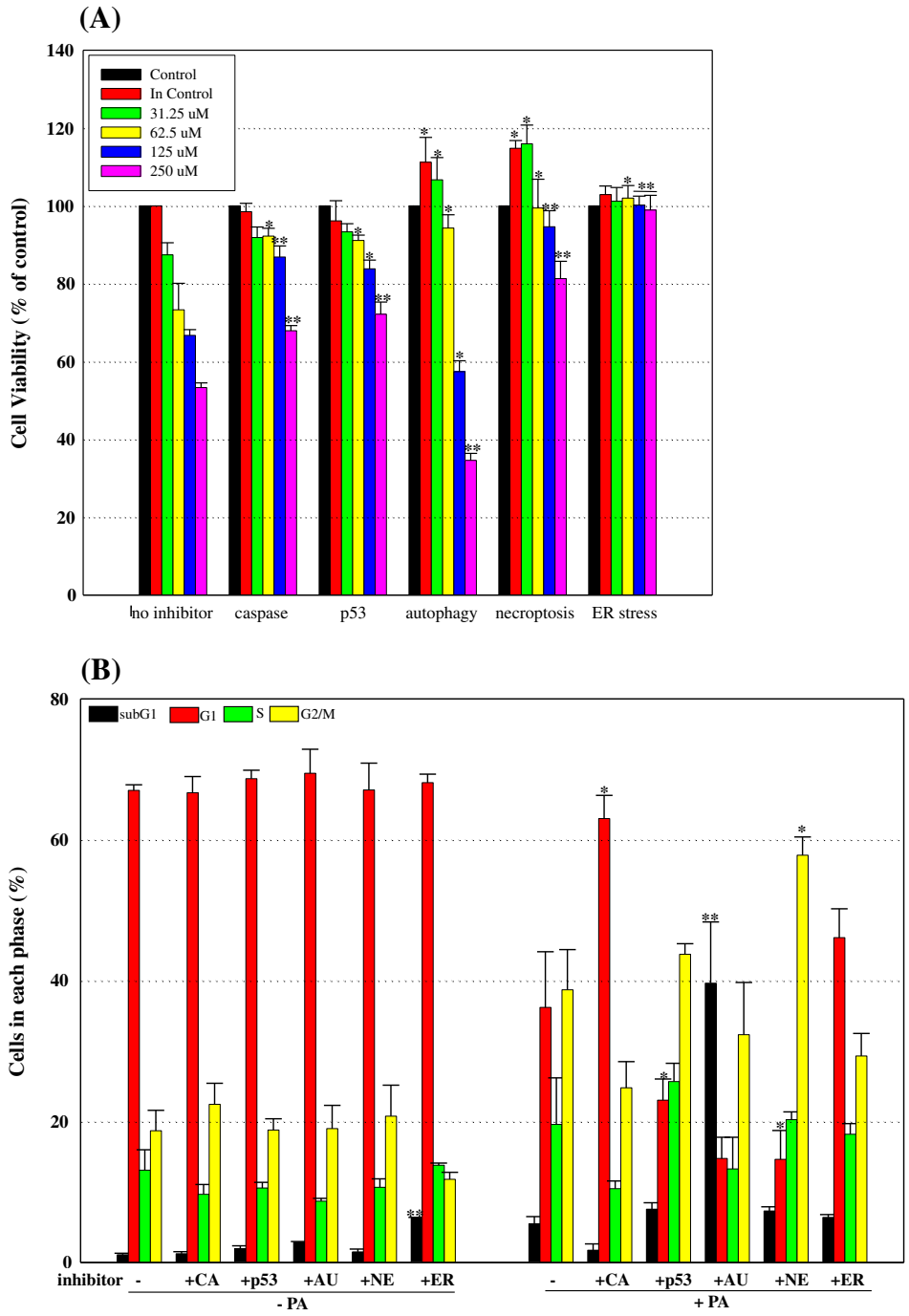

Fig. 7. Effects of various inhibitors on PA-induced alterations in cell viability and cell cycle. Cells were pretreated with inhibitors of caspase (CA, Z-VAD-FMK, 0.2 μM), p53 (pifithrin-alpha, 1 μM), autophagy (AU, Baf A1, 0.1 μM), and necroptosis (NE, necrostatin-1, 1 μM) for 1 h. Cells were also pretreated with an ER-stress inhibitor (ER, TUDCA, 200 μM) for 24 h. Experiments were performed 3 independent times, and in each experiment, 6 wells were used per concentration. The results are presented as AV ± SD. The statistical significance of inhibitor groups was evaluated based on the corresponding concentration of no-inhibitor group. $^{*}p < 0.05$; $^{**}p < 0.01$. (A) Effect on cell viability. Viability of the treatment group is expressed as a percentage of the control group, which was considered as 100%. (B) Effect on cell cycle.

Furthermore, when the fusion between autophagosomes and lysosomes was blocked, the ER became dilated and PA-induced morphological changes were exacerbated, which was accompanied by a disappearance of cellular components and an increase in apoptotic cell death. The PA-induced aggregation of p62 protein was also exacerbated after Baf A1 pretreatment.

Taken together, our results suggest that PA induces apoptosis accompanied by autophagy through mitochondrial dysfunction and ER stress that are triggered by oxidative stress in human Chang liver cells. Moreover, the impairment of autophagic function may accelerate cellular damage following PA exposure.

Conflict of Interest

We wish to confirm that there are no known conflicts of interest associated with this publication and there has been no significant

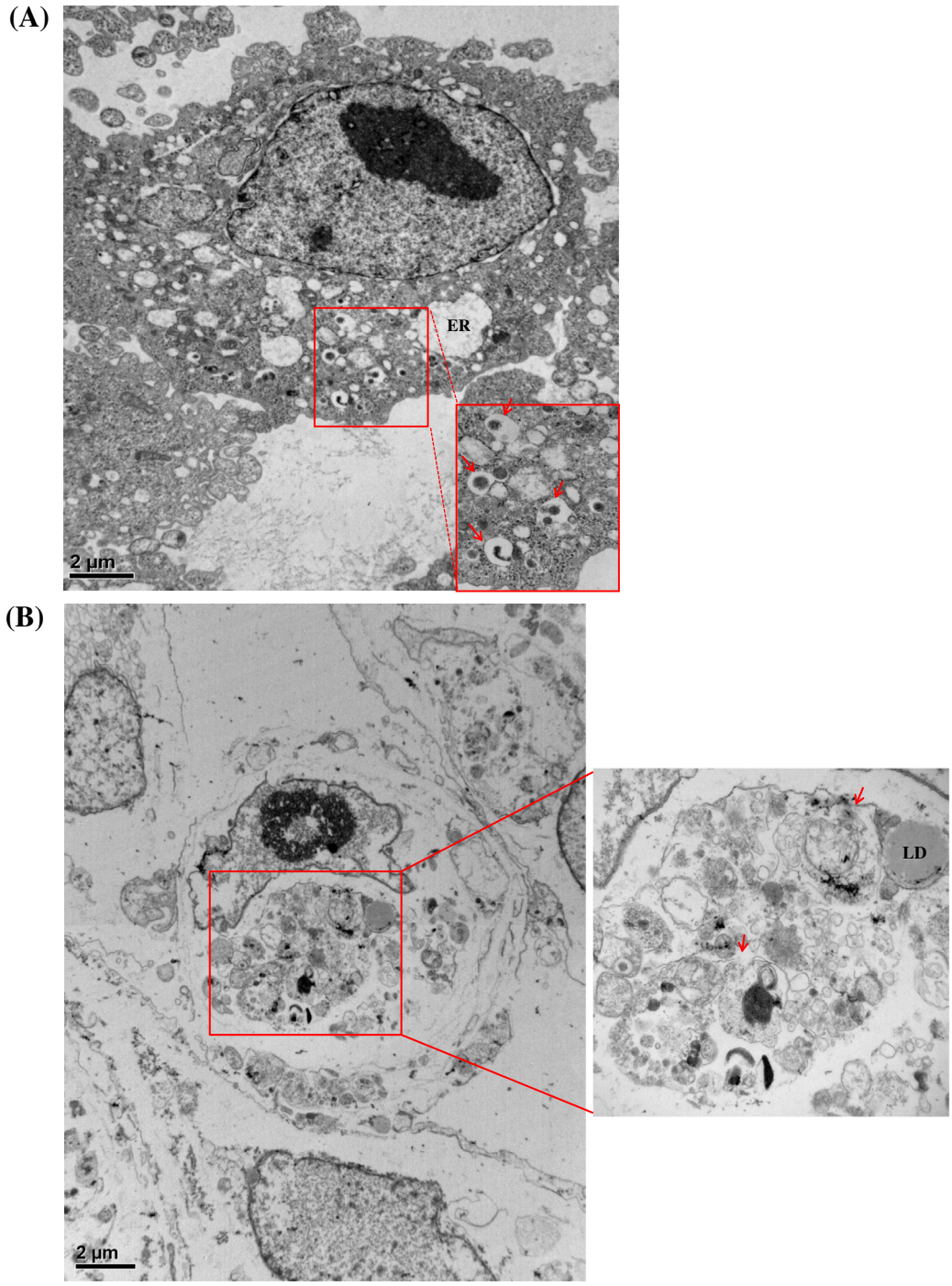

Fig. 8. Exacerbation of PA-induced morphological changes following Baf A1 pretreatment. Cells were pretreated with BaF A1 (1 h) and incubated without or with PA (250 μM) for 24 h. The red box shows a magnified image for clarity and the red arrows indicate autophagosome-like vacuoles. (A) Only Baf A1 treatment. The ER became dilated and autophagosome-like vacuoles increased. (B) PA exposure with Baf A1 pretreatment. Cell membranes and cellular components disappeared. (For interpretation of the references to colour in this figure legend, the reader is referred to the web version of this article.)

financial support for this work that could have influenced its outcome.

Transparency Document

The Transparency document associated with this article can be found in the online version.

Acknowledgements

This study was supported by the National Research Foundation (NRF) of Korea funded by the Ministry of Science, ICT & Future Planning (2012M3A9C4048819 and the Basic Science Research Program through the NRF of Korea funded by the Ministry of Education, Science, and Technology (2011-35B-E00011). M.H.C.

also acknowledges the support of the Veterinary Research Institute of Seoul National University in Korea. A.Y.L. and S.P. also acknowledge the support from BK21 Plus program.

Appendix A. Supplementary material

Supplementary data associated with this article can be found, in the online version, at http://dx.doi.org/10.1016/j.fct.2014.01.027.

References

Basu, A., Haldar, S., 1998. The relationship between Bcl2, Bax and p53: consequencs for cell cycle progression and cell death. Mol. Hum. Reprod. 4 (12), 1099–1109.

Cao, J., Dai, D.L., Yao, L., Yu, H.H., Ning, B., Zhang, Q., Chen, J., Cheng, W.H., Shen, W., Yang, Z.X., 2012. Saturated fatty acid induction of endoplasmic reticulum stress and apoptosis in human liver cells via the PERK/ATF4/CHOP signaling pathway. Mol. Cell Biochem. 364 (1–2), 115–129.

Chaabane, W., User, S.D., El-Gazzah, M., Jaksik, R., Sajjadi, E., Rzeszowska-Wolny, J., Los, M.J., 2013. Autophagy, apoptosis, mitoptosis and necrosis: interdependence between those pathways and effects on cancer. Arch. Immunol. Ther. Exp. (Warsz) 61 (1), 43–58.

Chen, X., Yin, X.M., 2011. Coordination of autophagy and the proteasome in resolving endoplasmic reticulum stress. Vet. Pathol. 48 (1), 245–253.

Choi, S.E., Lee, S.M., Lee, Y.J., Li, L.J., Lee, S.J., Lee, J.H., Kim, Y., Jun, H.S., Lee, K.W., Kang, Y., 2009. Protective role of autophagy in palmitate-induced INS-1 beta-cell death. Endocrinology 150 (1), 126–134.

Cox, T.M., Cachón-González, M.B., 2012. The cellular pathology of lysosomal diseases. J. Pathol. 226 (2), 241–254.

Dedukhova, V.I., Mokhova, E.N., Skulachev, V.P., Starkov, A.A., Arrigoni-Martelli, E., Bobyleva, V.A., 1991. Uncoupling effect of fatty acids on heart muscle mitochondria and submitochondrial particles. FEBS Lett. 295 (1–3), 51–54.

Ferri, K.F., Kroemer, G., 2001. Organelle-specific initiation of cell death pathways. Nat. Cell Biol. 3 (11), E255–E263.

Fukai, T., Ushio-Fukai, M., 2011. Superoxide dismutases: role in redox signaling, vascular function, and diseases. Antioxid. Redox. Signal. 15 (6), 1583–1606.

Gaggini, M., Morelli, M., Buzzigoli, E., DeFronzoi, R.A., Bugianesi, E., Gastaldelli, A., 2013. Non-alcoholic fatty liver disease (NAFLD) and its connection with insulin resistance, dyslipidemia, atherosclerosis and coronary heart disease. Nutrients 5 (5), 1544–1560.

Gu, X., Li, K., Laybutt, D.R., He, M.L., Zhao, H.L., Chan, J.C., Xu, G., 2010. Bip overexpression, but not CHOP inhibition, attenuates fatty-acid-induced endoplasmic reticulum stress and apoptosis in HepG2 liver cells. Life Sci. 87 (23–26), 724–732.

Imoto, Y., Yoshida, Y., Yagisawa, F., Kuroiwa, H., Kuroiwa, T., 2011. The cell cycle, including the mitotic cycle and organelle division cycles, as revealed by cytological observations. J. Electron. Microsc. (Tokyo) 60 (Suppl. 1), S117–S136.

Jin, S., 2005. P53, autophagy and tumor suppression. Autophagy 1 (3), 171–173.

Kim et al., 2006. Role of mitochondria as the gardens of cell death. Cancer Chemother. Pharmacol. 57 (5), 545–553.

Knævelsrud, H., Simonsen, A., 2012. Lipids in autophagy: constituents, signaling molecules and cargo with relevance to disease. Biochim. Biophys. Acta 1821 (8), 1133–1145.

Kroemer, G., Galluzzi, L., Vandenabeele, P., Abrams, J., Alnemri, E.S., Baehrecke, E.H., et al., 2009. Classification of cell death: recommendations of the nomenclature committee on cell death 2009. Cell Death Differ. 16 (1), 3–11.

Leamy, A.K., Egnatchik, R.A., Young, J.D., 2013. Molecular mechanisms and the role of saturated fatty acids in the progression of non-alcoholic fatty liver disease. Prog. Lipid Res. 52 (1), 165–174.

Lee, Y.Y., Hong, S.H., Lee, Y.J., Chung, S.S., Jung, H.S., Park, S.G., Park, K.S., 2010. Tauroursodeoxycholate (TUDCA), chemical chaperone, enhances function of islets by reducing ER stress. Biochem. Biophys. Res. Commun. 397 (4), 735–739.

Li, Z., Shi, K., Guan, L., Cao, T., Jiang, Q., Yang, Y., Xu, C., 2010. ROS leads to MnSOD upregulation through ERK2 translocation and p53 activation in selenite-induced apoptosis of NB4 cells. FEBS Lett. 584 (11), 2291–2297.

Liu, Czaja, 2013. Regulation of lipid stores and metabolism by lipophagy. Cell Death Differ. 20 (1), 3–11.

Liu, J., Minemoto, Y., Lin, A., 2004. C-Jun N-terminal protein kinase 1 (JNK1), but not JNK2, is essential for tumor necrosis factor alpha-induced c-Jun kinase activation and apoptosis. Mol. Cell Biol. 24 (24), 10844–10856.

Loria, P., Lonardo, A., Anania, F., 2013. Liver and diabetes. A vicious circle. Hepatol. Res. 43 (1), 51–64.

Lorin, S., Pierron, G., Ryan, K.M., Codogno, P., Djavaheri-Mergny, M., 2010. Evidence for the interplay between JNK and p53-DRAM signaling pathways in the regulation of autophagy. Autophagy 6 (1), 153–154.

Mei, S., Ni, H.M., Manley, S., Bockus, A., Kassel, K.M., Luyendyk, J.P., Copple, B.L., Ding, W.X., 2011. Differential roles of unsaturated and saturated fatty acids on autophagy and apoptosis in hepatocytes. J. Pharmacol. Exp. Ther. 339 (2), 487–498.

Moscat, J., Diaz-Meco, M.T., 2009. P62 at the crossroads of autophagy, apoptosis, and cancer. Cell 137 (6), 1001–1004.

Murea, M., Freedman, B.I., Parks, J.S., Antinozzi, P.A., Elbein, S.C., Ma, L., 2010. Lipotoxicity in diabetic nephropathy: the potential role of fatty acid oxidation. Clin. J. Am. Soc. Nephrol. 5 (12), 2373–2379.

Park, E.J., Yi, J., Chung, K.H., Ryu, D.Y., Choi, J., Park, K., 2008. Oxidative stress and apoptosis induced by titanium dioxide nanoparticles in cultured BEAS-2B cells. Toxicol. Lett. 180 (3), 222–229.

Park, E.J., Yi, J., Kim, Y., Choi, K., Park, K., 2010. Silver nanoparticles induce cytotoxicity by a Trojan-horse type mechanism. Toxicol. In Vitro 24 (3), 872–878.

Renault, T.T., Manon, S., 2011. Bax: addressed to kill. Biochimie 93 (9), 1379–1391.

Ricchi, M., Odoardi, M.R., Carulli, L., Anzivino, C., Ballestri, S., Pinetti, A., Fantoni, L.I., Marra, F., Bertolotti, M., Banni, S., Lonardo, A., Carulli, N., Loria, P., 2009. Differential effect of oleic and palmitic acid on lipid accumulation and apoptosis in cultured hepatocytes. J. Gastroenterol. Hepatol. 24 (5), 830–840.

Rivard, A.L., Steer, C.J., Kren, B.T., Rodrigues, C.M., Castro, R.E., Bianco, R.W., Low, W.C., 2007. Administration of tauroursodeoxycholic acid (TUDCA) reduces apoptosis following myocardial infarction in rat. Am. J. Chin. Med. 35 (2), 279–295.

Sano, R., Reed, J.C., 2013. ER stress-induced cell death mechanisms. Biochim Biophys Acta Epub ahead of print.

Schönfeld, P., Wojtczak, L., 2008. Fatty acids as modulators of the cellular production of reactive oxygen species. Free Radic. Biol. Med. 45 (3), 231–241.

Singh, R., Cuervo, A.M., 2012. Lipophagy: connecting autophagy and lipid metabolism. Int. J. Cell Biol. 2012, 282041.

Smaili, S.S., Pereira, G.J., Costa, M.M., Rocha, K.K., Rodrigues, L., do Carmo, L.G., Hirata, H., Hsu, Y.T., 2013. The role of calcium stores in apoptosis and autophagy. Curr. Mol. Med. 13 (2), 252–265.

Tanida, I., 2011. Autophagosome formation and molecular mechanism of autophagy. Antioxid. Redox. Signal. 14 (11), 2201–2214.

Vousden, K.H., Ryan, K.M., 2009. P53 and metabolism. Nat. Rev. Cancer 9 (10), 691–700.

Wu, W., Liu, P., Li, J., 2012. Necroptosis: an emerging form of programmed cell death. Crit. Rev. Oncol. Hematol. 82 (3), 249–258.

Zhang, X.D., Qin, Z.H., Wang, J., 2010. The role of p53 in cell metabolism. Acta Pharmacol. Sin. 31 (9), 1208–1212.

Zhang, Y., Xue, R., Zhang, Z., Yang, X., Shi, H., 2012. Palmitic and linoleic acids induce ER stress and apoptosis in hepatoma cells. Lipids Health Dis. 11, 1.